01

Transformation of the valence Si−O vibrations of smectite under effect of adsorbed $CaSO_4$ and H_2O molecules

© A.V. Morozov, A.G. Kochur, V.L. Shapovalov, M.V. Okost, V.A. Yavna

The Rostov State Transport University,
344038 Rostov-on-Don, Russia

e-mail: cpd@rgups.ru

Received June 06, 2023
Revised November 13, 2023
Accepted February 28, 2024

This work deals with experimental and theoretical investigation of the spectral properties of smectite, and its mixture with alabaster (building gypsum) at low moistures. The position and intensity of infrared spectrum bands at wave numbers in the range of $800-1250\,cm^{-1}$ coming from Si−O vibrations are investigated. In order to interpret the experimental spectra obtained by frustrated total internal reflection method, theoretical models based on DFT with XLYP-correlation potential are used, with cluster approximation for the smectite surface. This allowed determining optimal positions of the atoms of $CaSO_4$ and H_2O molecules near the basal surface. Positions and intensities of components of the IR spectra of clusters are calculated. The profile of water valence bands was calculated as superposition of Gaussian curves with the widths estimated from the experiment. Theoretical studies explained the observed transformations of spectral bands (variation of positions and intensities) resulting from the modification of the surface properties of smectite particles, and from changes in samples moisture. The agreement achieved in the positions and profiles of experimental and theoretical spectral bands justifies the adequacy of the theoretical description of modification of smectite properties, and the effect of hydration

Keywords: Infrared spectrum, DFT method, basal surface modification, cluster method, electron and spatial structure.

DOI: 10.61011/EOS.2024.02.58442.5289-23

Introduction

Soft clays have low strength and high compressibility, which results in significant settlements and failures of soils under application of mechanical loads [1–5]. Improvement of the soft clay properties appears to be a quite relevant task for many construction and transport objectives[6–9].

The solution to this problem may be related to the application, for example, of vacuumizing, thermal treatment, complexing etc. [10], which results in change of the microscopic properties of soils (shape and size of clayey particles, pore volume etc.), improves strength properties and reliability of earth structures.

Another method to modify the properties of soft clays is the mechanism of changing the properties of basal surfaces of clayey minerals by adsorption of chemical compounds with the wide spectrum of properties: fly ash, sand, basalt fiber [11] or cement [12]. The properties of modified surfaces are currently studied by experimental and theoretical methods of IR spectroscopy. The method of IR spectroscopy makes it possible to study both electronic and spatial structures of hydrated minerals, and to perform the quantitative analysis of the mineral composition of soils [13,14]. The results of the study of the IR spectra of the clayey soils make it possible to calculate a wide spectrum of mechanical properties, including the properties of plasticity and characteristics of shrinkage and ductility [15–17]. Experimental research of the IR spectra of the moistened montmorillonite STx-1b was performed in refs. [18,19] by the method of attenuated total reflectance (ATR). This method has proven itself well when solving the problems of qualitative and quantitative analysis [20]. The performed research made it possible to numerically evaluate the spectral features reflecting the formation of the water molecule layers on clayey particles. In particular, the abnormal position of the maximum and the value of the bandwidth of the valent oscillations of water were discovered at low moistures related to variation of the spatial structure due to the formation of the chemical bonding with the atoms of basal surfaces. Generalization of the research results made in ref. [21] made it possible to conclude that in the case of interaction of the clayey minerals with water molecules the ion-dipole and hydrogen bonds are formed. Active centers of adsorption may be formed due to the presence of the exchange ions near the surfaces of the clayey particles [22,23]. If there are no exchange ions, the points of adsorption are inside the rings made of six oxygen atoms.

Among the theoretical methods for calculation of interaction of individual molecules with clayey particles, Hartree-Fock methods [24] and methods based on the density functional theory (DFT) are usually used [25]. Simulation of hydration of the clayey particles with the basal surfaces of non-ideal shape and under the conditions of high moisture content is usually performed by the methods of molecular dynamics [26].

The purpose of this paper consists in the studying, using methods of experimental IR spectroscopy and quantum chemistry, the features of adsorption of molecules $CaSO_4$ and H_2O by basal surfaces of smectite, and in investigating the effect of the modification of the properties of basal surfaces on the formation of the IR spectrum bands in the wave number range of $800-1250\,cm^{-1}$. The interval of low moisture values is analyzed, with the upper limit of less than 20%. This made it possible to investigate, using the theoretical ab initio methods, the experimentally registered transformation of bands upon variation of moisture and additional adsorption of $CaSO_4$ molecules.

The selected range of wave numbers reflects valent oscillations Si−O which may characterize the properties of the smectite surfaces upon their modification. The results obtained in the paper will make it possible to expand the assortment of components that enable stabilization or modification of the physical and mechanical characteristics of soil materials, to improve the technology for preparation of modified soils and to monitor its quality. The results of the studies may be useful for making changes and additions to the regulatory documentation in the field of industrial and transport construction. At the same time the results of experimental research may serve as the basis for further theoretical studies of the interaction between the soil-forming minerals and alabaster.

Materials

Experimental studies

As a clayey material for research, bentonite of grade „Kutch“ was chosen. This material was produced at the commercial deposit located in the Kutch region, West India. The studies of the chemical composition of bentonite of grade „Kutch“ were performed in refs. [27–29]. Concentrations of the most significant chemical compounds in bentonite of grade „Kutch“ are given in the ref. [30]. It is noted in [31] that the considered bentonite may contain up to 80% smectite in the form of montmorillonite (Kutch BF 04) and beideliite (Kutch BF 08). The main difference of these clays is observed in the capacity of the cation exchange. The choice of this clayey material is related to high content of montmorillonite and wide sphere of its application [32–34]. The properties of the clayey particles surfaces were modified by alabaster ($CaSO_4 \cdot 0.5H_2O$) [35,36]. This material was obtained as a result of thermal treatment of a natural gypsum dihydrate $CaSO_4 \cdot 2H_2O$ at temperature $150 - 180^\circ C$ in the units open to atmosphere. For experimental research, the samples are used which were produced by mixing bentonite and alabaster that were first dried to constant mass according to [37] and ground in a ball mill. The mass of the dry mix of bentonite and alabaster is determined by the relation

$$M = m + m_B = 1.3m_B, \quad (1)$$

where M is the mass of dry mix, m is the mass of alabaster equal to 30% of the bentonite mass (m_B).

For experimental research, the moistened samples of bentonite and alabaster mix were used with moisture content W. The moistened samples were prepared by adding distilled water, the mass of which is determined by the relation

$$m_{H_2O} = WM/100, \quad (2)$$

where m_{H_2O} is the mass of added water, W is the necessary moisture content of the sample in percent, M is the mass of dry mix.

Theoretical studies

The crystalline structure of smectite is initially built based on the experimental data provided at http://rruff.geo.arizona.edu/AMS/amcsd.php (American Mineralogist Crustal Structure Database, database_code_amcsd 0012237). The siloxane basal surface of smectite was simulated in cluster approximation. The cluster of the basal surface contained silicon atoms and surrounding oxygen tetrahedrons. The chemical bonds of atoms broken when building the clusters were closed with hydrogen atoms. Use of this cluster model for qualitative interpretation of the spectra is justified in the ref. [24], where the IR spectrum transformation is interpreted in case of kaolinite moisture variation using *ab initio* simulation. As alabaster ($CaSO_4 \cdot 0.5H_2O$) and water molecules, molecules $CaSO_4$ and H_2O were used in the calculations.

Methods

Study of infrared spectra

The infrared spectra of samples were studied at temperature 23°C using the method of attenuated total reflectance (ATR) with application of IR Fourier spectrometer Alpha (Bruker Optik GmbH, Ettlingen, Germany).

Infrared spectra are measured in the middle infrared range from 500 to $4000\,cm^{-1}$ using software OPUS (Bruker Optics GmbH, Ettlingen, Germany). Spectra were measured using the module Alpha-E. Registering mode: averaging over 50 scans, resolution — $2\,cm^{-1}$. The natural surface of the sample placed on the surface of ZnSe crystal was studied.

Calculation of the spatial position of atoms

To simulate the atomic structure of clusters, the DFT method was used [38–40]. To calculate the electronic states and correlations in the clusters, the triply „degenerated“ McLean-Chandler basis set was used supplemented with polarization functions: two functions of *p*-symmetry and one function of *d*-symmetry [41]. Optimization of atoms positions and calculations of the cluster properties are made using the suite Firefly v.8.2.0 [42], which is partially based on the source code GAMESS [43]. The calculations used

the exchange-correlation functional XLYP, used previously in the ref. [44] as the optimal when calculating the spectral characteristics in the objects of similar atom composition. Upon implementation of the numerical procedure, the convergence limits of the electron density and energy of the self-consistent field were chosen to be 0.00001. Upon optimization of the spatial positions, the iterations stopped when the change in the values of the energy gradient vector components became less than 0.000003. At such degree of optimization, the error in determination of wave numbers is usually below 10 cm^{-1}. The structure of the clusters is visualized using software suite MacMolPlt v 7.7 [45].

Calculation of wave numbers and intensities of oscillations

Wave numbers and intensities of oscillations in IR spectra of clusters were calculated in harmonic approximation. The choice of approximation is related to a good agreement of theoretical values of the wave numbers in the spectrum of the H_2O molecule with the experiment and to minor variation of the accuracy of calculated values upon transition to the anharmonic approximation. In particular, for molecule H_2O the theoretical values of the wave numbers of valent and deformation oscillations differ from the experimental ones by less than 0.3%. The transition to the anharmonic approximation changes the values of the wave numbers by less than 0.2%, and intensities — by less than 10%. The transition from the harmonic approximation to the anharmonic approximation in the process of calculating the wave numbers and intensities of oscillations in the molecule $CaSO_4$, consisting of heavier atoms, results in the change of these values by 1 and 5%, accordingly. These values may be assumed the estimates of harmonic approximation accuracy when researching the oscillations Si–O in bentonite.

Formation of the shape of valent bands of water in the spectra of moistened samples

When simulating the shapes of the oscillation bands in the studied clusters, it is assumed that individual oscilatory states appear in the IR spectra in the form of Gaussian-shaped profiles. The profiles of the clusters spectra bands are calculated by summing the Gaussian components in respective spectral regions. The widths of Gaussian components are taken to be identical — they were evaluated experimentally and made 35 cm^{-1} [35].

Study results

Infrared spectra

Fig. 1 shows normalized spectra of dry samples of bentonite, alabaster, and the mix of bentonite and alabaster. The spectra are normalized in accordance with SNV (standard normal variate) algorithms.

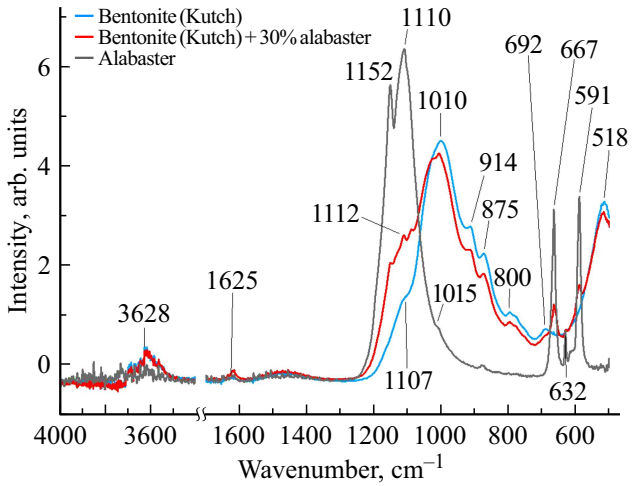

Figure 1. Infrared absorption spectra of dry samples: bentonite Kutch (blue), alabaster (black) and the mix of bentonite and alabaster (red).

The infrared spectrum of bentonite (Kutch) indicates that montmorillonite is a dominant mineral phase in this clay [46]. The bands 3628 and 1625 cm^{-1} are due to valent and deformation oscillations of the OH-groups of montmorillonite [46,47]. Low intensity of these bands is due to the fact that the samples are dried to constant mass. However, in the spectrum they are present due to the availability of small residues of free and bound water. The bands 914 and 875 cm^{-1} comply with the deformation oscillations of montmorillonite groups: Al-Al-OH, Al-Fe-OH [46,48–55]. The intensive band 800 cm^{-1} can be attributed to the lamellar form of disordered tridymite [48,51,54], and the band 692 cm^{-1} — to the presence of quartz in the sample [48,49,54]. Valent oscillations Si-O of smectite produce a complex wide band 1150–1000 cm^{-1} [46,48,51,53–55]. Ref. [56] relate the absorption in the spectrum area below 550 cm^{-1} with the planar oscillations of octahedral ions and adjacent oxygen layers. Therefore, the split band in the spectrum near 518 cm^{-1} may be observed as a result of combined oscillations that may be related to symmetric valent oscillations Me-O or deformation oscillations Si-O with the same probability. Thus, the works [46,54] relate the band 518 cm^{-1} to deformation oscillations Si-O-Al. At the same time, the work [55], referring to [56], suggests that the absorption band 518 cm^{-1} and the closely lying band 494 cm^{-1} arise as a result of deformation oscillations Si-O-Si and translational modes of octahedral ions and adjacent oxygen layers.

In the spectrum of dry alabaster it is possible to identify the most intense bands 1152, 1110 cm^{-1}, which reflect the antisymmetric modes of valent oscillations of tetrahedrons SO_4 [57–62]. At the same time, the mode of symmetric valent oscillations ν_1 (SO_4) is compliant with a very weak band 1015 cm^{-1} [57,59,60]. In the case of a fully symmetric octahedron such oscillations may not show themselves in the IR spectrum since they do not cause formation of a

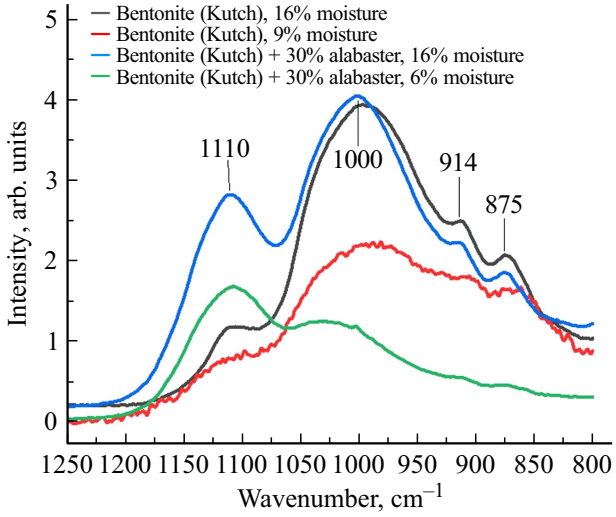

Figure 2. Infrared absorption spectra of moistened samples: bentonite Kutch (grey — moisture 16%, red — moisture 9%), mix of bentonite and alabaster (blue — moisture 16%, green — moisture 6%).

dipole moment. Availability of a weak-intensity band at 1015 cm^{-1}, therefore, indicates a certain distortion of the SO_4 octahedron geometry in alabaster.

Also characteristic os alabaster are the bands with wave numbers 667, 632 and 591 cm^{-1} which comply with the modes of antisymmetric deformation oscillations of SO_4 [57–61]. The presence of residual water in the dry alabaster may be detected and characterized by the bands in the spectral regions of around 3600–3500 and 1600 cm^{-1} [57,58,60,61]. Band intensities in these regions are low and significantly noisy. The presence of residual water in the dried sample indicates poor quality of sample preparation.

The spectrum of the bentonite and alabaster mix sample contains the bands of main oscillations of bentonite, and normal oscillations of $CaSO_4$ molecules — the main component of alabaster.

To study the spectral region corresponding to the transformation of valent Si–O oscillations of smectite when under effect of adsorbed molecules $CaSO_4$ and H_2O, the corresponding IR measurements are made in the moistened samples. Their spectra are shown in Fig. 2.

A more detailed analysis of respective intervals of IR spectra is provided below.

Calculation results

Calculations of optimal position of atoms in the clusters containing fragments of siloxane basal surface included definition of the position of six atoms of silicon and twelve surface atoms of oxygen belonging to central tetrahedrons, as well as of atoms within molecules $CaSO_4$ and H_2O. Coordinates of other atoms of the clusters remained the same. Positions of the hydrogen atoms closing the chemical bonds broken when building the cluster of the smectite surface were frozen after optimization of atoms in the surface cluster.

Total energies and binding energies of molecules and clusters studied in this paper

Clusters	Total energy, a.u.	Binding energy, eV	Binding energy of water, eV
Ca	−677.728		
SO_4	−699.245		
$CaSO_4$	−1377.206	6.34	
H_2O	−76.487		
Cluster A (fragment of basal surface of smectite, Fig. 3, *a*)	−6202.105		
Ca+Cluster A	−6879.838	0.15	
SO_4+Cluster A	−6901.395	1.24	
$CaSO_4$+Cluster A	−7579.407	2.68	
H_2O+Cluster A	−6278.599		0.22
H_2O+$CaSO_4$+Cluster A	−7655.939	3.93	1.23

The results of calculation of spatial positions of atoms in clusters is shown in Fig. 3.

In Fig. 3, *b* it is seen that in absence of the exchange ions near the surface of smectite (Fig. 3, *a*) the adsorption points of the molecule H_2O are in the rings of six atoms of oxygen, which is compliant with the data of [16]. In Fig. 3, *c* it is seen that the atom Ca of the molecule $CaSO_4$ is placed in the center of the hexagon formed by tetrahedrons made of oxygen atoms. At the same time, due to the tendency of the group of atoms SO_4 to be arranged near the tetrahedron, the water molecule is pushed off. It should be noted that in areas of localization of $CaSO_4$ there is no formation of a water layer directly interacting with the basal surface of smectite (Fig. 3, *d*).

The table shows energy characteristics of atoms, molecules and clusters obtained as a result of optimization of spatial positions of atoms. The given values of total energies of multi-atom systems are used to calculate the energies of bonding between the molecules $CaSO_4$ and H_2O and separately the energy of bonding of the molecule H_2O on the basal surface of smectite.

Comparison of the results of experimental and theoretical studies

Fig. 4 compares theoretical and experimental bands of IR absorption spectra of smectite with various moistures.

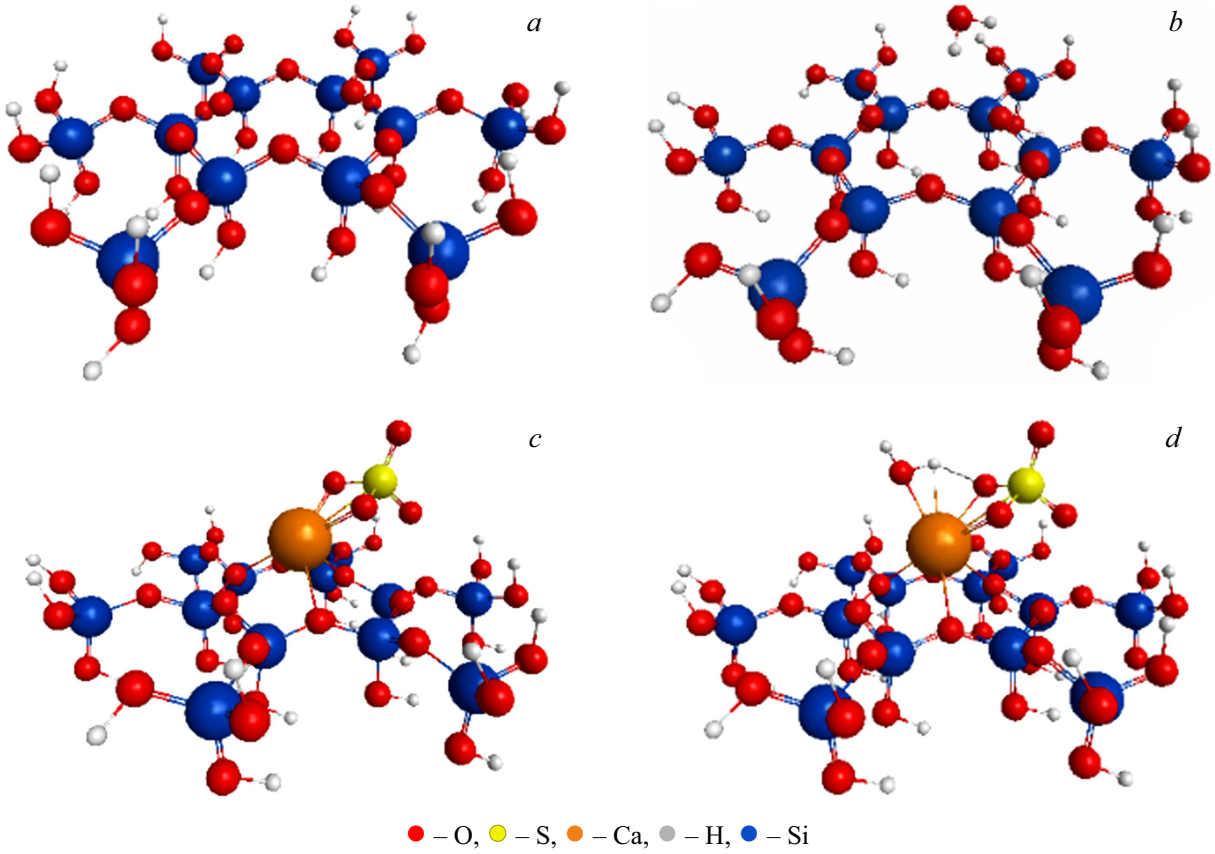

Figure 3. Optimal position of the atoms included in molecules H_2O (*b*), $CaSO_4$ (*c*), $CaSO_4$ and H_2O (*d*) near the fragment of the basal surface of smectite (*a*).

Theoretical spectral bands are calculated for the clusters shown in Fig. 3, *a* and 3, *b*.

Fig. 5 compares theoretical and experimental bands of IR absorption spectra of smectite and alabaster mix with various moistures. Theoretical spectral bands are calculated for the cluster shown in Fig. 3, *d*.

Discussion of the results

The data given in the table make it possible to conclude that the binding energy energy of the molecule $CaSO_4$ in the free state is 6.34 eV. With optimal placement of the molecule near the basal surface of smectite, the binding energy reduces down to 2.68 eV, which gives reason to assume the preservation of the molecular structure during adsorption of $CaSO_4$. Indeed, the placement of atom Ca and SO_4 group near the basal surface of smectite reduces the bond energy down to 1.39 eV. At the same time the molecule stretches along the direction of the chemical bond between Ca and S, and the distance between the atoms increases from 2.857 to 2.893 A. Hence it appears that in the spectroscopic studies it is first of all necessary to optimize the position of the molecule $CaSO_4$ near the smectite surface, not considering separately the optimization of the positions of Ca and SO_4. However, the objective of separate optimization of positions of Ca and SO_4 may arise in cases of high moisture of samples, when dissociation of $CaSO_4$ near the basal surface of smectite may be related to formation of solvation shells. Special calculation demonstrated that the addition of one molecule H_2O increases the distance between Ca and S from 2.893 to 2.9837 A.

The binding energy of water molecule (0.22 eV), calculated in the absence of the exchange ions and given in the table, is well matched to the value 0.26 eV from [22]. The binding energy of water molecules increases significantly after the modification of surface properties during adsorption of $CaSO_4$. In this case the binding energy increases up to 1.23 eV. This is due to the formation of a chemical bond between molecules $CaSO_4$ and H_2O, as shown in Fig. 3, *d*.

Bands in the range of wave numbers 800–1250 cm^{-1}

Let us consider the behavior of two bands with wave numbers near 1000 and 1110 cm^{-1} shown in Fig. 4. As the moisture of the bentonite samples reduces, the intensity of these bands decreases, and the peak intensity of the first of them exceeds the peak intensity of the second one in the entire range of used moistures. The noted pattern may be explained by the reduction of water molecule concentration

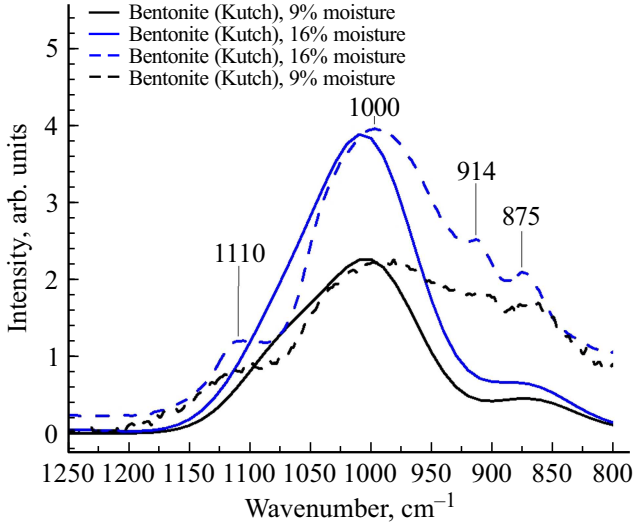

Figure 4. Theoretical (solid curves) and experimental (dashed curves) bands of IR absorption spectra of smectite with various moistures: 9% — black curves, 16% — blue curves.

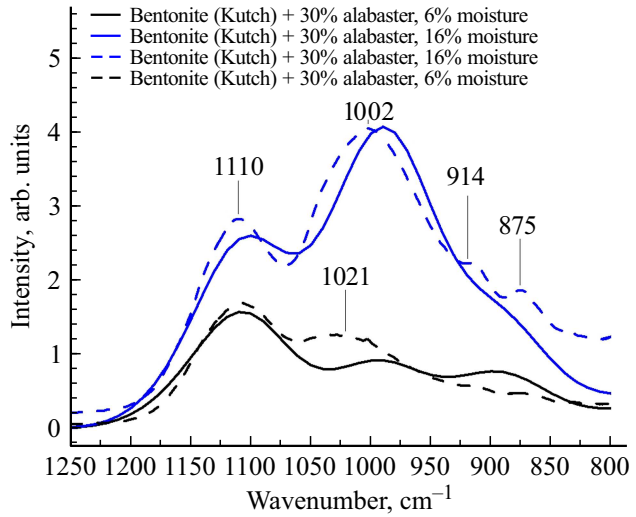

Figure 5. Theoretical (solid curves) and experimental (dashed curves) bands of IR absorption spectra of smectite and alabaster mix with various moistures: 6% — black curves, 16% — blue curves.

near the surface of clayey particles affecting the valent oscillations of Si–O.

The spectra displayed in Fig. 5 show that the reduction of moisture in the mixes of bentonite and alabaster also results in simultaneous reduction in the intensity of these bands, however, in this case the band with the wave number 1110 cm^{-1} becomes more intense, compared to that in bentonite without additional admixtures. Increased intensity of the band at 1110 cm^{-1} may be due to the manifestation of valent oscillations of molecules $CaSO_4$ — the main component of alabaster. The wave numbers of these oscillations are calculated in [35] and are equal to 1053 and 1184 cm^{-1}, and in the measured spectra of dry alabaster given in Fig. 1, they are noted at wave numbers 1152, 1110, 1015 cm^{-1}. At low moistures, the peak intensity of the band 1110 cm^{-1} exceeds the peak intensity of the band 1021 cm^{-1}. Besides, as the moisture increases, a complex wide band forms in the wave number region near 1002 cm^{-1}, which may be explained by modification of the properties of smectite basal surfaces due to adsorption of $CaSO_4$ and additional adsorption of water molecules by the $CaSO_4$ molecules.

Comparison of the profiles and positions of theoretical and experimental bands of smectite of various moisture given in Fig. 4, makes it possible to note that the theory reproduces the main features of the experiment. In particular, two experimental bands with wave numbers 875 and 914 cm^{-1} appear in the calculation in the form of a single wide band. The experimental band with wave number 1110 cm^{-1} appears in the theory in the form of a bulge on the band with the wave number 1021 cm^{-1}. The main disadvantage of the theory may be the insufficient intensity of the theoretical spectrum in the range of wave numbers 800–1000 cm^{-1}. This deviation, however, may be related to inaccuracy of background subtraction when processing the experimental spectra.

Comparison of the profiles and positions of theoretical and experimental bands of smectite modified by alabaster as given in Fig. 5 makes it possible to note their good agreement for the considered moistures of samples. As in the case of smectite, two experimental bands with wave numbers 875 and 914 cm^{-1} appear in the calculation in the form of a single wide band. The theory reproduces well the advanced growth of the intensity of the band with the wave number of around 1000 cm^{-1} at the growth of moisture and the ratio of peak intensities of bands with the wave numbers 1000 and 1110 cm^{-1}.

Conclusions

Adsorption of water and alabaster molecules on the basal surfaces of clayey particles of smectite results in simultaneous changes in the electronic and spatial structure of the interacting objects. To study them, this paper used the cluster approximation in simulation of the basal surfaces of smectite and molecules adsorbed on it. Calculations of the optimal position of cluster atoms are made in the DFT approximation using McLean-Chandler (MC) basic set supplemented with polarization functions: two functions of *p*-symmetry and one of *d*-symmetry. Besides, it was obtained that upon the adsorption of the molecule of $CaSO_4$ on the smectite surface the binding energy of Ca and SO_4 fragments reduces more than 4 times, and the distance between Ca and S atoms increases. Addition of one molecule H_2O in the cluster results in increase of this distance, which makes it possible to assume possible dissociation of the $CaSO_4$ molecule upon formation of solvation shells at high moistures.

Modification of the smectite surface properties related to the adsorption of $CaSO_4$ and H_2O is reflected in the transformation of the IR spectra bands. The performed theoretical studies of the profiles of the bands with wave numbers 1000 and 1110 cm^{-1} in the smectite-water and smectite-alabaster systems made it possible to interpret experimentally observed reduction of peak intensities of the bands in the first case and inversion of peak intensities in the second one.

Funding

This study was supported by the Russian Science Foundation (grant № 21-79-20005).

Conflict of interest

The authors declare that they have no conflict of interest.

References

[1] H. Tahershamsi, R. Ahmadi-Naghadeh, B. Zuada-Coelho, J. Dijkstra. Transportation Geotechnics, **42**, 101011 (2023). DOI: 10.1016/j.trgeo.2023.101011

[2] T. Zhang, T. Li, S. Feng. Soil Dynamics and Earthquake Engineering, **166**, 107727 (2023). DOI: 10.1016/j.soildyn.2022.107727

[3] H. Lei, M. Liu. Soil Dynamics and Earthquake Engineering, **153**, 107086 (2022). DOI: 10.1016/j.soildyn.2021.107086

[4] Y. Zheng, H. Sun, M. Hou, X. Ge. Engineering Geology, **293**, 106284 (2021). DOI: 10.1016/j.enggeo.2021.106284

[5] V.I. Osipov. *Priroda prochnostnykh i deformatsionnykh svoystv glinistykh porod* (Izd-vo MGU, M., 1979). (in Russian) https://search.rsl.ru/ru/record/01007707371

[6] S. Li, D. Wang, C. Tang, Y. Chen. Construction and Building Materials, **374**, 130902 (2023). DOI: 10.1016/j.conbuildmat.2023.130902

[7] A.L. Ramírez, L. Korkiala-Tanttu. Transportation Geotechnics, **38**, 100920 (2023). DOI: 10.1016/j.trgeo.2022.100920

[8] A.M. Omar, S.S. Agaiby, M.A. EL-Khouly. Ain Shams Engineering Journal, **15** (3), 102500 (2023). DOI: 10.1016/j.asej.2023.102500

[9] V.V. Sirotyuk, E.N. Alkaev, A.A. Lunev. *Sb. materialov IV Mezhdunarodnoy nauchno-prakticheskoy konferentsii: Arkhitekturno-stroitelny i dorozhno-transportny kompleksy: problemy, perspektivy, innovatsii* (Sibirsky gosudarstvenny avtomobilno-dorozhny universitet (SibADI), Omsk, 2019), s. 329−334. (in Russian) https://www.elibrary.ru/download/elibrary_42386891_78408791.pdf

[10] D.T. Bergado, S. Chaiyaput, S.Artidteang, T. Nghia-Nguyen. Geotextiles and Geomembranes, **48** (6), 828-843 (2020). DOI: 10.1016/j.geotexmem.2020.07.003

[11] Q. Ma, Z. Cao, Y. Pu. Advances in Materials Science and Engineering, **2018**, 9125127 (2018). DOI: 10.1155/2018/9125127

[12] Z. Cao, Q. Ma, H. Wang. Advances in Civil Engineering, **2019**, 8214534 (2019). DOI: 10.1155/2019/8214534

[13] S. Kaufhold, M. Hein, R. Dohrmann, K. Ufer. Vibrational Spectroscopy, **59**, 29−39 (2012). DOI: 10.1016/j.vibspec.2011.12.012

[14] A. Morozov, A. Vasilchenko, A. Kasprzhitskii, G. Lazorenko, V. Yavna, A. Kochur. Vibrational Spectroscopy, **114**, 03258 (2021). DOI: 10.1016/j.vibspec.2021.103258

[15] B.K. Waruru, K.D. Shepherd, G.M. Ndegwa, P.T. Kamoni, A.M. Sila. Biosystems Engineering, **121**, 177−185 (2014). DOI: 10.1016/j.biosystemseng.2014.03.003

[16] M. Knadel, H. Ur Rehman, N. Pouladi, L. Wollesen de Jonge, P. Moldrup, E. Arthur. Geoderma, **402**, 115300 (2021). DOI: 10.1016/j.geoderma.2021.115300

[17] M. Davari, S.A. Karimi, H.A. Bahrami, S.M. Taher Hossaini, S. Fahmideh. CATENA, **197**, 104987 (2021). DOI: 10.1016/j.catena.2020.104987

[18] T.F. Nazdracheva, A.V. Kukharskii, A.S. Kasprzhitskii, G.I. Lazorenko, V.A. Yavna, A.G. Kochur. Opt. Spectrosc., **129**, 270−275 (2021). DOI: 10.1134/S0030400X21020107

[19] A.A. Vasilchenko, I.A. Kondrashov, D.V. Olkhovatov. *Sb. nauchnykh trudov: Mezhdunarodnoy nauchno-prakticheskoy konferentsii: Aktualnye problemy i perspektivy razvitiya transporta, promyshlennosti i ekonomiki Rossii* (Rostovsky gosudarstvenny universitet putey soobscheniya, Rostov-na-Donu, 45−48 (2020). (in Russian)

[20] M. Ritz, L. Vaculikova, E. Plevova. Acta Geodynamica et Geomaterialia, **8**, 1 (161), 47−58 (2011). https://www.irsm.cas.cz/materialy/acta_content/2011_01/4_Ritz.pdf

[21] R.A. Schoonheydt, C.T. Johnston. Developments in Clay Science, **1**, 87−113 (2006). DOI: 10.1016/S1572-4352(05)01003-2

[22] C. Peng, F. Min, L. Liu, J. Chen. Applied Surface Science, **387**, 308−316 (2016). DOI: 10.1016/j.apsusc.2016.06.079

[23] A.-A. Abd-Elshafi, A.A. Amer, A. El-Shater, E.F. Newair, M. El-rouby. J. Molecular Liquids, **383**, 122092 (2023). DOI: 10.1016/j.molliq.2023.122092

[24] V. Yavna, T. Nazdracheva, A. Morozov, Y. Ermolov, A. Kochur. Crystals, **11** (9), 1146 (2021). DOI: 10.3390/cryst11091146

[25] X. Hu, A. Michaelides. Surface Science, **602** (4), 960−974 (2008). DOI: 10.1016/j.susc.2007.12.032

[26] R. Šolc, M.H. Gerzabek, H. Lischka, D. Tunega. Geoderma, **169**, 47−54 (2011). DOI: 10.1016/j.geoderma.2011.02.004

[27] R.K. Takoo, B.R. Patel. Crystal Research and Technology, **21** (1), 141−144 (1986). DOI: 10.1002/crat.2170210134

[28] R.R. Pawar, Lalhmunsiama, H.C. Bajaj, S.-M. Lee. J. Industrial and Engineering Chemistry, **34**, 213−223 (2016). https://doi.org/10.1016/j.jiec.2015.11.014

[29] A.S. Semenkova, M.V. Evsiunina, P.K. Verma, P.K. Mohapatra, V.G. Petrov, I.F. Seregina, M.A. Bolshov, V.V. Krupskaya, A.Yu. Romanchuk, S.N. Kalmykov. Applied Clay Science, **166**, 88−93 (2018). DOI: 10.1016/j.clay.2018.09.010

[30] A. Morozov, A. Vasilchenko, V. Shapovalov, A. Kochur, V. Yavna. Transportation Research Procedia, **68**, 947−954 (2023). DOI: 10.1016/j.trpro.2023.02.132

[31] S. Olsson, O. Karnland. *Characterisation of bentonites from Kutch, India and Milos, Greece — some candidate tunnel back-fill materials?* (SKB Rapport R-09-53, 2009). https://inis.iaea.org/collection/NCLCollectionStore/_Public/41/038/41038317.pdf

[32] S. Pu, Z. Zhu, W. Huo. Conservation and Recycling, **174**, 105780 (2021). DOI: 10.1016/j.resconrec.2021.105780
[33] D. Toksöz Hozatlıoğlu, I. Yılmaz. Engineering Geology, **280**, 105931 (2021). DOI: 10.1016/j.enggeo.2020.105931
[34] Ahmed Usama H. Issa. Soils and Foundations, **54** (3), 405–416 (2014). DOI: 10.1016/j.sandf.2014.04.009
[35] A.V. Morozov, D.V. Olkhovatov, V.L. Shapovalov, A.G. Kochur, V.A. Yavna. Izv. Sarat. Univ. Novaya Seriya. (in Russian). Seriya: Fizika, **23** (3), 221–237 (2023). (in Russian)
DOI: 10.18500/1817-3020-2023-23-3-221-237
[36] A. Morozov, V. Shapovalov, Y. Popov, A. Kochur, V. Yavna. Vibrational Spectroscopy, **128**, 103582 (2023).
DOI: 10.1016/j.vibspec.2023.103582
[37] GOST 5180-2015. *Grunty. Metody laboratornogo opredeleniya fizicheskikh kharakteristik* (Standartinform, M., 2016). (in Russian)
[38] E.K.U. Gross, R.M. Dreizler. *Density Functional Theory: An Approach to the Quantum Many-Body Problem* (Springer US, 2013). DOI: 10.1007/978-1-4757-9975-0
[39] N. Bork, L. Du, H. Reiman, T. Kurtén, H.G. Kjaergaard. J. Physical Chemistry A, **118** (28), 5316–5322 (2014).
DOI: 10.1021/jp5037537
[40] A.G. Shklovsky, A.V. Beregovoy. *Teoriya funktsionala elektronnoy plotnosti dlya atomov i prostykh molekul* (ID „Belgorod“ NIU „BelGU“, Belgorod, 2014). (in Russian)
[41] E. Magnusson. J. Computational Chemistry, **14** (1), 54–66 (1993). DOI: 10.1002/jcc.540140110
[42] A.A. Granovsky. Firefly. version 8 [Electronic source]. http://classic.chem.msu.su/gran/firefly/index.html
[43] M.W. Schmidt, K.K. Baldridge, J.A. Boatz, S.T. Elbert, M.S. Gordon, J.H. Jensen, S. Koseki, N. Matsunaga, K.A. Nguyen, S. Su, T.L. Windus, M. Dupuis, J.A. Montgomery. J. Computational Chemistry, **14** (11), 1347–1363 (1993). DOI: 10.1002/jcc.540141112
[44] Morozov, T. Nazdracheva, A. Kochur, V. Yavna. Spectrochimica Acta Part A, **287** (2), 122119 (2023).
DOI: 10.1016/j.saa.2022.122119
[45] B.M. Bode, M.S. Gordon. J. Molecular Graphics and Modelling, **16** (3), 133–138 (1998).
DOI: 10.1016/S1093-3263(99)00002-9
[46] J. Madejová, J. Kečkéš, H. Pálková, P. Komadel. Clay Minerals, **37** (2), 377–388 (2002).
DOI: 10.1180/0009855023720042
[47] S.Yu. Khashirova, Z.L. Beslaneeva, I.V. Musov, Yu.I. Musaev, A.K. Mikitaev. Fundamentalnye issledovaniya, **8** (1), 202–206 (2011). (in Russian)
https://fundamental-research.ru/ru/article/view?id=26814
[48] B. Tyagi, Ch.D. Chudasama, R.V. Jasra. Spectrochimica Acta Part A, **64** (2), 273–278 (2006).
DOI: 10.1016/j.saa.2005.07.018
[49] A.G. Chetverikova, V.N. Makarov, O.N. Kanygina, M.M. Seregin, V.L. Berdinsky, A.V. Kanaki, E.S. Deeva, A.A. Smorokov, M.S. Syrtanov, E.B. Gello. ZhTF, **94** (1), 99–108 (2024). (in Russian) DOI: 10.61011/JTF.2024.01.56907.167-23
[50] J.D. Russell, V.C. Farmer, B. Velde. Mineralogical Magazine, **37** (292), 869–879 (1970).
DOI: 10.1180/minmag.1970.037.292.01
[51] G.E. Christidis, P.W. Scott, A.C. Dunham. Applied Clay Science, **12** (4), 329–347 (1997).
DOI: 10.1016/S0169-1317(97)00017-3
[52] J.D. Russell, A.R. Fraser. *Infrared methods*. In: Wilson M.J. (eds) *Clay Mineralogy: Spectroscopic and Chemical Determinative Methods* (Springer, Dordrecht, 1994).
DOI: 10.1007/978-94-011-0727-3_2
[53] K. Bukka, J.D. Miller, J. Shabtai. Clays Clay Miner., **40**, 92–102 (1992). DOI: 10.1346/CCMN.1992.0400110
[54] J. Madejová, P. Komadel, Clays Clay. Miner., **49**, 410–432 (2001). DOI: 10.1346/CCMN.2001.0490508
[55] G. Jovanovski, P. Makreski. Macedonian J. Chemistry and Chemical Engineering, **35** (2), 125–155 (2016).
DOI: 10.20450/mjcce.2016.1047
[56] V.C. Farmer, J.D. Russell. Spectrochimica Acta Part A, **20** (7), 1149–1173 (1964). DOI: 10.1016/0371-1951(64)80165-X
[57] 10. L. Yang. Planetary and Space Science, **163**, 35–41 (2018).
DOI: 10.1016/j.pss.2018.04.010
[58] M. Hass, G.B.B.M. Sutherland. Proc. Roy. Soc. Lond., **236**, 427–445 (1956). DOI: 10.1098/rspa.1956.0146
[59] E. Melliti, K. Touati, B. van der Bruggen, H. Elfil. Chemosphere, 263, 127866 (2021).
DOI: 10.1016/j.chemosphere.2020.127866
[60] Janice L. Bishop, Melissa D. Lane, M. Darby Dyar, Sara J. King, Adrian J. Brown, Gregg A. Swayze. American Mineralogist, **99** (10), 2105–2115 (2014).
DOI: 10.2138/am-2014-4756
[61] A.V. Naumov, A. V. Sergeeva. *Sb. trudov pyatoy nauchno-tekhnicheskoy konferentsii: K 100-letiyu organizatsii instrumentalnykh seismologicheskikh nablyudeniy na Kamchatke „Problemy kompleksnogo geofizicheskogo monitoringa Dalnego Vostoka Rossii“* (Federalny issledovatelsky tsentr ”Edinaya geofizicheskaya sluzhba Rossiyskoy akademii nauk”, Obninsk, 2015) s. 86–90. (in Russian)
https://elibrary.ru/item.asp?id=25678520
[62] K. Nakamoto. *IK spectry i spektry KR neorganicheskikh i koordinatsionnykh soedinenii* (Mir, M., 1991). (in Russian)

Translated by M.Verenikina